



**HAL**  
open science

## Inverse ARX (IARX) method for boundary specification in heat conduction problems

A. v. s. Oliveira, C. Zacharie, Benjamin Remy, Vincent Schick, D. Maréchal,  
Julien da Costa Teixeira, S. Denis, Michel Gradeck

► **To cite this version:**

A. v. s. Oliveira, C. Zacharie, Benjamin Remy, Vincent Schick, D. Maréchal, et al.. Inverse ARX (IARX) method for boundary specification in heat conduction problems. *International Journal of Heat and Mass Transfer*, 2021, 180, pp.121783. 10.1016/j.ijheatmasstransfer.2021.121783 . hal-03444243

**HAL Id: hal-03444243**

**<https://hal.univ-lorraine.fr/hal-03444243>**

Submitted on 1 Dec 2022

**HAL** is a multi-disciplinary open access archive for the deposit and dissemination of scientific research documents, whether they are published or not. The documents may come from teaching and research institutions in France or abroad, or from public or private research centers.

L'archive ouverte pluridisciplinaire **HAL**, est destinée au dépôt et à la diffusion de documents scientifiques de niveau recherche, publiés ou non, émanant des établissements d'enseignement et de recherche français ou étrangers, des laboratoires publics ou privés.



Distributed under a Creative Commons Attribution - NonCommercial - NoDerivatives 4.0  
International License

# Inverse ARX (IARX) method for boundary specification in heat conduction problems

A. V. S. Oliveira<sup>a,b,c</sup>, C. Zacharie<sup>b</sup>, B. Rémy<sup>b</sup>, V. Schick<sup>b</sup>, D. Maréchal<sup>a</sup>, J. Teixeira<sup>c,d</sup>, S. Denis<sup>c,d</sup>, M. Gradeck<sup>b,\*</sup>

<sup>a</sup>*IRT M2P, 4 rue Augustin Fresnel 57070 Metz, France*

<sup>b</sup>*Université de Lorraine, CNRS, LEMTA, F-54000 Nancy, France*

<sup>c</sup>*Institut Jean Lamour, UMR 7198 CNRS, Université de Lorraine, Nancy, France*

<sup>d</sup>*Laboratory of Excellence “Design of Alloy Metals for Low-mass Structures” (DAMAS), Univ. Lorraine, Nancy, France*

---

## Abstract

Heat conduction problems are usually solved either with analytical or numerical simulations, or with a reduced model using system identification. The use of polynomial models, often used in automation theory, gained the attention of the thermal community in the last decades to elaborate these reduced models because of their simplicity and performance to characterize an invariable system. They allow, for example, estimating a local temperature with a known input heat source. However, using polynomial models (or identified systems) in inverse conduction problems is not straightforward, usually requiring either a second inversion step. In this paper, we present a novel inverse technique based on the polynomial model ARX (autoregressive with exogenous input) that allows the estimation of an unknown input (like an imposed heat flux on a boundary) using a known output (temperature measurement). This new method, named inverse ARX or IARX, only requires a calibration step as a regular polynomial model and, then, it can estimate the input by a direct calculation with the identified parameters. The difference between IARX and ARX is the presence of future exogenous parameters, which were deduced using the initial discrete form of the ARX model. We present herein a numerical example using IARX of a 1D heat conduction simulation and IARX succeeded to estimate the input heat flux, even with high discontinuities and high measurement noises. Finally, we compare the proposed method with the classical Beck’s function specification method. IARX presented advantages like having no restriction for the number of future terms used in the method and performing the calculation 45% faster and with much less memory space consumption than with Beck’s method.

*Keywords:*

Inverse method, Parametric models, Polynomial models, System identification, Exogenous, Autoregressive, Future time steps

---

## Nomenclature

### Greek Letters

		$\phi$	heat flux
$\alpha$	thermal diffusivity	$\rho$	density
$\lambda$	thermal conductivity	$\sigma$	standard deviation

---

\*Corresponding author

*Email address:* michel.gradeck@univ-lorraine.fr (M. Gradeck)

$\Theta$	temperature difference	L	length
$\varepsilon$	noise	n	number of a parameter
<b>Roman Letters</b>		p	Laplace parameter
<b>A</b>	past-input sub-matrix	r	relative residue
<b>B</b>	past-output sub-matrix	T	temperature
<b>C</b>	future-output sub-matrix	t	time
<b>d</b>	result vector	u	input
<b>p</b>	parameters vector	X	thermal impedance
<b>S</b>	sensitivity matrix	x	position
<b>u</b>	input vector	y	output
a	autoregressive parameter	Z	inverse Laplace solution
b	past exogenous parameter	<b>Subscripts</b>	
c	future exogenous parameter	f	future
$c_p$	specific heat	fts	future time steps
fit	fit parameter	p	past
H	impulse response	ref	referential
k	time step	TC	thermocouple

## 1. Introduction

In most engineering applications, we find cases of a generic system excited with an input  $u$  providing a response or output  $y$  (Fig. 1) [1], like a base excitation of a body-spring-damper system resulting in the body displacement, a voltage input giving an electrical current output, or a heat power changing the temperature field in a body. Looking to describe the target system as best as possible, engineers develop methods to predict the output ( $y_{mo}$ ) using a known input and a model for the system, this calculation being usually referred to as direct problem. However, there are as well applications where the output is known by measurements and we desire to find the input that caused that response. This is known as inverse problem, as the developed model is used in the "opposite sense". The issue with this last method is that these models are usually ill-posed, which means that measurement noises and model errors are amplified during inversion and diverges the input calculation, requiring the use of regularization methods.

This paper focuses exactly on this problem for heat transfer applications of estimating unknown boundary conditions varying in time from the knowledge of one or several temperature evolution data in a space domain. This is a classical inverse heat conduction problem (IHCP) whose resolution applies to situations with a heat power, heat flux, or temperature source (input) that stimulates a homogeneous material system and results in the observed or measured temperature response (output). We find many examples of IHCP solved using different functional minimization techniques, like the Generalized Minimal Residual Method (GMRES, which is basically a least squares tool)

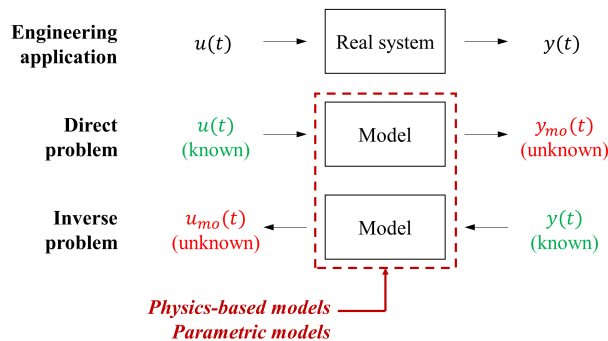


Figure 1: Input-output relations in a real engineering application and its modeling for direct and inverse problems.

[9], Bayesian approaches [10, 11] or the PID-control theory [12]. We must allude to Beck's major contribution on IHCP [2, 3], including non-linear problems [4], and particularly for his function specification method that processes the ill-posed nature of the corresponding inverse problem. Other popular regularization techniques based on some type of modified least square technique can also be underlined: Tikhonov's method [5, 6], truncated singular value decomposition (TSVD) [7, 8].

As mentioned before, a reliable model is required to be used in the inverse algorithm and, then, correlate the input and the output (Fig. 1). A strictly analytical model is achievable for cases with simple geometries, known physical properties and defined measurement location, although it hardly corresponds exactly to the real system being studied. Otherwise, problems with complex geometries or boundary conditions require using a detailed model based on a spatial discretization, which allows extracting input-output correlations that can be described by so-called reduced models. If the system studied is linear time-invariant (LTI), these reduced models are a convolution product, as dictated by Duhamel's theorem [13], which means the transient temperature behavior at any location in the domain can be written in continuous time  $t$  using the superposition principle as follows:

$$y(t) = \sum_{i=1}^{n_u} \int_0^t u_i(t - \tau) H_i(\tau) d\tau \quad (1)$$

where  $y(t)$  is the output temperature response at time  $t$  and at a given point in the system,  $u_i(t)$  is the amplitude of the  $i$ -th thermal input,  $n_u$  is the number of inputs in the system, and  $H_i(t)$  the associated impulse response to the  $i$ -th source for the same point. Indeed, the impulse responses  $H_i(t)$  fully characterize the system model as they do not depend on the transient profile of the associated sources.

In order to perform such model reduction, or system identification if the data sets are directly provided by an experiment, the impulse responses can be estimated through polynomial models, intensively studied by Ljung [14]. More precisely, some forms of these parametric models (which are as well reduced models) can be considered as generalizations of impulse responses, and thus adapted to thermal behavior laws. Among them, autoregressive models with exogenous inputs (ARX) are very appropriate to represent input-output laws relating thermal flux and potentials due to their simplicity and performance. The discrete original structure of ARX models to calculate the output  $y$  at a time step  $k$  is given by:

$$y[k] = - \sum_{i=1}^{n_a} a_i y[k - i] + \sum_{i=0}^{n_b-1} b_i u[k - n_k - i] \quad (2)$$

where  $a_i$  and  $b_i$  are, respectively, the autoregressive and exogenous parameters,  $n_a$  and  $n_b$  their respective quantities, and  $n_k$  is the dead-time parameter, which can be used when there is a delay between the system response and the input. On the one hand, the need for exogenous parameters to estimate an output temperature is more evident because past thermal inputs are necessary for this calculation, as already shown with Duhamel's theorem in Eq. 1. On the other hand, the use of autoregressive parameters is less evident following Eq. 1. However, they are necessary because estimating the present output using previous ones, which are rich in information of past events, avoids the need of using all the previous inputs in the calculation. Thus, an ARX model with a few autoregressive and exogenous parameters could provide precise estimates of the current temperature output.

In the last decades, ARX models, which have always been useful in fields like mathematics and automation, gained attention as well in other applications, especially in thermal engineering. Buildings are an excellent example of the applied use of parametric models because of their complex shape and transient input sources. Milovanović et al. [15] and Jiménez et al. [16] used fit methods to estimate efficiently behavior laws for buildings, Mustafaraj et al. [17], Wu and Sun [18], and Ríos-Moreno et al. [19] used them to create virtual sensors, while Yu et al. [20] and Yoshida and Kumar [21] were able to improve the energy efficiency of some installations. Furthermore, parametric models are very appropriate to monitor industrial environments and equipment because of their fast response and relatively easy application [22–24]. Researchers have also dedicated efforts on augmented versions of these linear models [25–27].

Most of the applications cited above solve direct problems using parametric models, i.e. the input heat sources  $u(t)$  are known and the temperature outputs  $T(t)$  are estimated. In this case, one calibration step using an inverse method is necessary either to find the system response function  $H_i(t)$  or to obtain the reduced model parameters  $a_i$  and  $b_i$  (still considering a system that cannot be or is hardly modeled analytically). After that, the use of the parametric models to estimate the outputs with the known inputs is rather straightforward. Nevertheless, this is not the case when using classical methods to solve an IHCP, as shown in Fig. 2 (left). In such circumstance, after the calibration step (step 2 in the figure), another inverse method is necessary to estimate the input source with temperature measurements [25]. This implies using another regularization technique, which, consequently, increases the computational cost. For this reason, we propose herein a novel inversion method based on the original ARX model: the inverse ARX, or IARX, which uses only one inversion step during the calibration. After this step, it allows the source estimation by a direct calculation using the identified model, thus eliminating the second inversion step in classical methods (Fig. 2, right).

This paper is structured as follows. First, we introduce the IARX method from the original ARX discrete structure and recall the identification steps to obtain the reduced model parameters. Then, we present a numerical example of a 1D diffusive system, including the identification of an IARX structure that estimates directly the researched input heat flux. In the discussion, we analyze the effect of each IARX parameter on the inversion quality and stability. Finally, we compare the IARX performance with the classical Beck's function specification procedure.

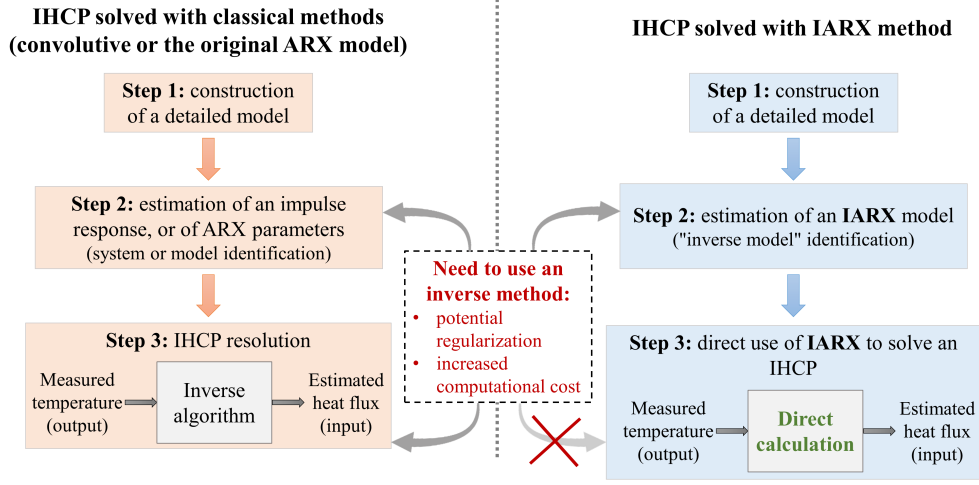


Figure 2: Comparison between the IHCP classical approach and the proposed Inverse ARX (IARX).

## 75 2. The Inverse ARX method (IARX)

### 2.1. Method presentation

To differentiate the original ARX and the proposed IARX parameters in the following equations, we used a prime symbol ( $'$ ) to represent those corresponding to the original ARX and no additional symbol for the novel IARX. Using Eq. 2 as a departure, the original ARX discrete structure can be rewritten as the following expression if we consider  
80 the existence of an autoregressive parameter  $a'_0$  to  $y[k']$  (for a time step  $k'$ ),  $n'_a + n_c + 1$  the number of autoregressive terms ( $n_a$  in Eq. 2),  $n'_b + n_c + 1$  the number of exogenous terms ( $n_b$  in Eq. 2), and neglect the presence of a response delay ( $n_k = 0$ ):

$$\sum_{i=0}^{n'_a+n_c} a'_i y[k' - i] = \sum_{i=0}^{n'_b+n_c} b'_i u[k' - i] \quad (3)$$

We can split the summations and obtain the equation:

$$\sum_{i=0}^{n_c-1} a'_i y[k' - i] + \sum_{i=n_c}^{n'_a+n_c} a'_i y[k' - i] = \sum_{i=0}^{n_c-1} b'_i u[k' - i] + b'_{n_c} u[k' - n_c] + \sum_{i=n_c+1}^{n'_b+n_c} b'_i u[k' - i] \quad (4)$$

that still allows the calculation of the output  $y[k']$ , which is included in the first summation in the left side of Eq. 4  
85 (when  $i = 0$ ). Nevertheless, we can use the same expression to calculate an intermediary input  $u[k] = u[k' - n_c]$  after changing the time step reference as shown in Fig. 3. Therefore, Eq. 4 becomes:

$$\sum_{i=1}^{n_c} a_{f,i} y[k + i] + \sum_{i=0}^{n'_a} a_{p,i} y[k - i] = \sum_{i=1}^{n_c} b_{f,i} u[k + i] + b_{n_c} u[k] + \sum_{i=1}^{n'_b} b_{p,i} u[k - i] \quad (5)$$

where the subscripts  $f$  and  $p$  refer to future and past parameters, either autoregressive and exogenous, in relation to the time step  $k$  in IARX. Because future inputs  $u[k + i]$  are still unknown while estimating the input  $u[k]$ , we can set  $b_{f,i} = 0$  for  $1 \leq i \leq n_c$  and, after rearranging the equation we find:

$$b_{n_c} u[k] = \sum_{i=1}^{n_c} a_{f,i} y[k + i] + \sum_{i=0}^{n'_a} a_{p,i} y[k - i] - \sum_{i=1}^{n'_b} b_{p,i} u[k - i] \quad (6)$$

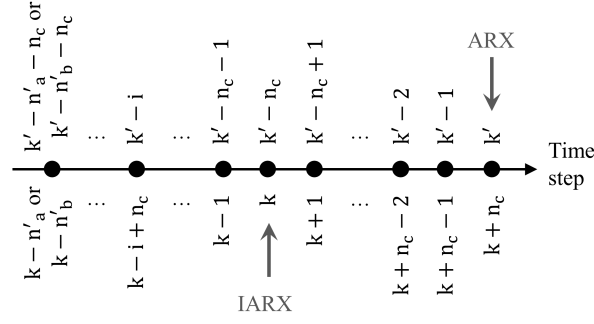


Figure 3: Change in the calculated time step from ARX to IARX.

90 Notice that we would obtain the same expression in Eq. 6 if we considered either  $u[k+i] = u[k]$  or  $u[k+i] = 0$  in Eq. 5, which means we are assuming a fixed value for future inputs. However, with transient inputs, this would create a biased estimation if  $n_c$  is large. We show in the results section this is not the case as the estimations are not biased even for very large  $n_c$ . Finally, we rename and recognize the role of each coefficient in this new IARX structure comparing with the original ARX equation. Therefore,  $b_{p,i}/b_{n_c} = a_i$  are actually the autoregressive parameters, 95  $a_{p,i}/b_{n_c} = b_i$  are the past exogenous parameters, and  $a_{f,i}/b_{n_c} = c_i$  are the future exogenous parameters. The notation for the number of each parameter is also corrected, i.e.  $n'_b = n_a$  is the number of autoregressive parameters,  $n'_a + 1 = n_b$  is the number of past exogenous parameters, and  $n_c$  is still the number of future exogenous parameters. This leads to the final equation of the proposed Inverse ARX (IARX) method given by:

$$u[k] = - \sum_{i=1}^{n_a} a_i u[k-i] + \sum_{i=0}^{n_b-1} b_i y[k-i] + \sum_{i=1}^{n_c} c_i y[k+i] \quad (7)$$

recalling that, in an IHCP,  $u$  is the thermal input to be estimated and  $y$  is the temperature response of the system.

100 This equation can be written as matrices and vectors:

$$\mathbf{u}_{(n_t-n_c,1)} = \mathbf{S}_{(n_t-n_c,n_p)} \mathbf{P}_{(n_p,1)} \quad (8)$$

$n_t$  being the number of collected data (number of time steps),  $\mathbf{u}$  the vector containing the estimated inputs,  $\mathbf{p}$  the IARX parameters vector, and  $\mathbf{S}$  the sensitivity matrix, which are respectively defined by:

$$\mathbf{u}_{(n_t,1)} = [u[1] \ u[2] \ \dots \ u[k] \ \dots \ u[n_t - n_c]]^T \quad (9)$$

$$\mathbf{P}_{(n_p,1)} = [a_1 \ a_2 \ \dots \ a_{n_a} \ b_0 \ b_1 \ \dots \ b_{n_b-1} \ c_1 \ c_2 \ \dots \ c_{n_c}]^T \quad (10)$$

$$\mathbf{S}_{(n_t,n_p)} = [\mathbf{A}_{n_t-n_c,n_a} \ \mathbf{B}_{n_t-n_c,n_b} \ \mathbf{C}_{n_t-n_c,n_c}] \quad (11)$$

where  $\mathbf{A}$ ,  $\mathbf{B}$  and  $\mathbf{C}$  are sub-matrices containing respectively the past inputs, past outputs and future outputs, that

is:

$$\mathbf{A}_{(n_t-n_c, n_a)} = \begin{bmatrix} 0 & 0 & \dots & 0 \\ -u[1] & 0 & \dots & 0 \\ -u[2] & -u[1] & \dots & 0 \\ \vdots & \vdots & \ddots & \vdots \\ -u[k-1] & -u[k-2] & \dots & -u[k-n_a] \\ \vdots & \vdots & \ddots & \vdots \\ -u[n_t-n_c-1] & -u[n_t-n_c-2] & \dots & -u[n_t-n_c-n_a] \end{bmatrix} \quad (12)$$

$$\mathbf{B}_{(n_t-n_c, n_b)} = \begin{bmatrix} y[1] & 0 & \dots & 0 \\ y[2] & y[1] & \dots & 0 \\ y[3] & y[2] & \dots & 0 \\ \vdots & \vdots & \ddots & \vdots \\ y[k] & y[k-1] & \dots & y[k-n_b+1] \\ \vdots & \vdots & \ddots & \vdots \\ y[n_t-n_c] & y[n_t-n_c-1] & \dots & y[n_t-n_c-n_b+1] \end{bmatrix} \quad (13)$$

$$\mathbf{C}_{(n_t-n_c, n_c)} = \begin{bmatrix} y[2] & y[3] & \dots & y[1+n_c] \\ y[3] & y[4] & \dots & y[2+n_c] \\ y[4] & y[5] & \dots & y[3+n_c] \\ \vdots & \vdots & \ddots & \vdots \\ y[k+1] & y[k+2] & \dots & y[k+n_c] \\ \vdots & \vdots & \ddots & \vdots \\ y[n_t-n_c+1] & y[n_t-n_c+2] & \dots & y[n_t] \end{bmatrix} \quad (14)$$

Hence, Eq. 7 allows to estimate the inputs  $\mathbf{u}$  given a set of known outputs  $\mathbf{y}$ . Note that Eq. 7 is the same as the original ARX if  $n_c = 0$  and if we isolate the output  $y[k]$ . In this study where we present the proposed method, we assume that the system starts in thermal equilibrium. More precisely, the system is at the same temperature of the environment and no heat input is applied before the experiment or simulation starts, so both the initial and boundary conditions are known for  $t \leq 0$ .

## 2.2. Calibration and validation steps

The first step for using either the traditional ARX method or the proposed IARX is finding the values of the autoregressive and exogenous parameters. This is accomplished during a calibration process using known data (we herein name them reference, so we have  $\mathbf{u}_{ref}$  for the input and  $\mathbf{y}_{ref}$  for the output), obtained by experimental measurements or numerical simulations, to construct the matrix  $\mathbf{S}$  in Eq. 11. Then, we employ the least-squares method with Eq. 8 to estimate the parameters vector  $\hat{\mathbf{p}}$  (the hat indicates that the parameters are estimated), as

shown below:

$$\hat{\mathbf{p}} = \left( \mathbf{S}^T \mathbf{S} \right)^{-1} \mathbf{S}^T \mathbf{u}_{ref} \quad (15)$$

In an ideal scenario where the input and the output are noiseless, the estimated parameters  $\hat{\mathbf{p}}$  would be equal to a theoretically exact solution that is intrinsic to the analyzed system. Nevertheless, because experimental measurements usually contain noise (which can be reproduced in numerical simulations), the estimated parameters might differ substantially from the exact solution. For this reason, it is important to reinforce that  $\hat{\mathbf{p}}$  is not an exact solution because it is affected by the noise level. Nevertheless, its expected value is still the exact solution if the signal noise  $\varepsilon$  is independent and identically distributed, i.e. its value probability follows a normal distribution with zero mean value and  $\sigma_\varepsilon^2$  variance.

The second step consists of validating the parametric model found during calibration. This is performed using a different set of known data, also by experiments or simulations, to progressively estimate the input  $\hat{\mathbf{u}}$  at each instant  $k$ . Consequently, each line of the estimated matrix  $\hat{\mathbf{A}}$  (Eq. 12) is built with the previous heat flux estimated values (i.e. for  $n_a$  time steps before  $k$ ), finally having an estimated sensitivity matrix  $\hat{\mathbf{S}}$  containing the estimated inputs  $\hat{\mathbf{u}}$  and the measured outputs  $\mathbf{y}_{ref}$ , therefore:

$$\hat{\mathbf{u}} = \hat{\mathbf{S}} \hat{\mathbf{p}} \quad (16)$$

The method validation is done using two parameters: the relative residue  $\mathbf{r}$  and the fit percentage. The first is the difference between the estimated and the reference values divided by the reference value and is calculated at each time step, giving:

$$r[k] = \frac{\hat{u}[k] - u_{ref}[k]}{u_{ref}[k]} \quad (17)$$

while the fit percentage is given by:

$$fit = 100 \left[ 1 - \frac{\sum_{k=1}^{n_t - n_c} (u_{ref}[k] - \hat{u}[k])^2}{\sum_{k=1}^{n_t - n_c} (u_{ref}[k] - \bar{\hat{u}})^2} \right] \quad (18)$$

$\bar{\hat{u}}$  being the mean value of  $\hat{\mathbf{u}}$ . While we desire  $r[k]$  to be as close as possible to zero, a 100% fit percentage means the parametric model represents perfectly the reference input, a 0% fit means that the obtained model is as accurate as a straight line over the mean value, and  $fit \rightarrow -\infty$  means the model reproduces poorly the known data.

### 2.3. Understanding the IARX method

If we compare the original ARX model (Eq. 2) and the proposed IARX (Eq. 7), we immediately observe that the autoregressive parameters ( $a_i$ ) play the same role of bringing past information from previously estimated values. This is not the case for the past exogenous parameter ( $b_i$ ). In the original ARX model, this parameter complies with the physics causality of past thermal inputs  $u$  affecting the present temperature output  $y$ , while in IARX it could be neglected because a present thermal input should not be dependent on past temperature responses. We show in the numerical application (section 3.3) that past exogenous parameters can indeed be suppressed without compromising substantially the thermal input estimate. The novelty found in IARX compared to ARX is the presence of future

exogenous terms, whose existence is reasonable if we think of the causality of the events. For a given time step  $k$ , only  
145 future temperature outputs  $y[k+i]$  are a response to the present thermal input  $u[k]$ . Therefore, they are certainly  
necessary to estimate the input, as well as autoregressive terms, as we demonstrated in section 3.3.

The reader who is familiarized with Beck's function specification method (FSM) [2], which is presented in detail  
in Appendix A based on our test case in section 3, would possibly recall the use of future temperature measurements  
to estimate a thermal input, like a heat flux as a boundary condition. His method uses the so-called future time  
150 steps, that is, uses  $n_{fts}$  future temperature measurements and consider a functional form for the  $n_{fts}$  future thermal  
inputs. The simplest approach is to consider these future inputs equal to the one being calculated at the time step  
 $k$ . Consequently, we have  $n_{fts}$  equations to estimate  $u[k]$ , whose value is found by least squares.

Even though  $n_{fts}$  in Beck's FSM and  $n_c$  in IARX are the number of future data used to estimate the present  
input, they are conceptually different from each other. Beck's future time steps act as a filter for the temperature  
155 noise, thus the higher the  $n_{fts}$ , the higher the filtering action, reducing the problem with the signal noise. However,  
an excessive increase in  $n_{fts}$  can bias the thermal input estimate because the functional form adopted for the future  
thermal inputs, like a constant value, deviates from reality. In turn, the future exogenous parameters in IARX are  
the output responses to previous inputs, hence using a higher  $n_c$  means having more information to estimate the  
present thermal input. Therefore, we should not expect any biasing because of the choice of  $n_c$ , although it still  
160 must not be excessive so IARX would start modeling the noise as well. Despite this conceptual difference, both  
methods need future output information to estimate the current input, which means  $n_{fts}$  and  $n_c$  play the same role  
in an engineering application of the number of necessary future measurements to solve the inverse problem. This  
parameter may affect, for example, the response delay in onboard diagnosis applications, as we demonstrated in the  
last section of the numerical application example (section 3.4).

In the introduction, we mentioned the use of detailed models, like an analytical solution with Duhamel's theorem  
165 (Eq. 1), or reduced models, like the proposed IARX, to solve an IHCP. Both approaches provide prior information  
to solve an inverse problem, the first using a physical or an identified model, and the second using a calibration step  
with known input and output to find the input-output correlation through autoregressive and exogenous parameters.  
Notice that, before IARX calibration step, we may not have complete information of the system, which is the reason  
170 for using parametric models. Nevertheless, identifying and developing simplified models the involved phenomena  
may provide useful information to identify the system inputs that affect a target output, so the obtained parametric  
model would be more robust. After the calibration step is performed, the identified IARX parameters allow solving  
the inverse problem with the direct calculation of the thermal input (as shown in Fig. 2) with Eq. 7 using measured  
temperature outputs. Therefore, the inputs and outputs identification and the calibration step are very important  
175 to mitigate the information deficit of the IHCP.

Finally, it is important to observe the applicability of the proposed IARX method in real experiments, especially  
during the calibration step. Measuring a temperature response is normally evident in an experiment, but the thermal  
input (for example, heat flux at a boundary) is usually not easy or even impossible to measure. This was already  
challenging even for classical IHCPs but it is feasible in controlled experiments, like using plate heater on a boundary  
180 and thermal insulation as performed by Beck et al. [3]. Even though Al Hadad et al. [28] performed a numerical study  
of a heat exchanger, it could be easily reproduced experimentally because the thermal input is an inlet temperature.

In cases where the experimental evaluation of the thermal input is unfeasible, detailed numerical simulations of the experiment can help to identify input-output correlations or validate the inverse method [9, 29], so they are also an option to generate data for the calibration step and find the IARX parameters.

### 185 3. Numerical application and discussion

#### 3.1. Test case presentation

Figure 4 presents the test case we used to generate the input and output data for the model calibration and validation by solving the heat equation. This is a simple 1D transient heat conduction problem in a planar wall with a variable heat flux  $\phi(0, t) = \phi$  applied onto the wall at  $x = 0$  and insulated surface at  $x = L$ . A temperature probe  
 190 is located at  $x_{TC}$  and its measurements are used as the output of our system, while the heat flux  $\phi$  is the thermal input we desire to obtain with the IARX method. With  $\alpha$  being the material thermal diffusivity, the heat equation to solve is:

$$\frac{\partial^2 T}{\partial x^2} = \frac{1}{\alpha} \frac{\partial T}{\partial t} \quad (19)$$

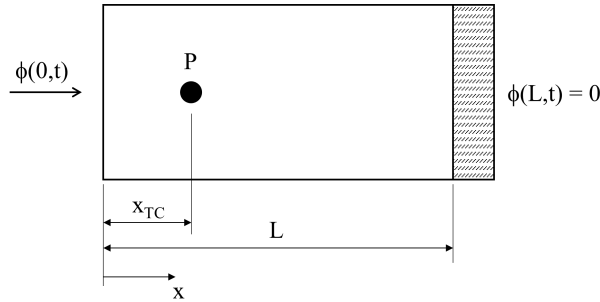


Figure 4: Tested case: 1D transient heat conduction in a planar wall.

The analytical solution that gives the temperature at the probe location is obtained using the quadrupoles method [30] and considering the heat flux input as constant by parts (Duhamel's theorem) [13], we find the analytical solution  
 195 in the discrete form as presented below:

$$\Theta[k] = \sum_{j=0}^{k-1} X_{k-j} \phi[j] \quad (20)$$

where  $\Theta_k$  is the difference between the probe temperature at the time step  $k$  and the initial temperature, and  $\mathbf{X}$  is the impedance vector whose elements are calculated by:

$$X_j = -\frac{1}{\lambda} \int_{t_j}^{t_{j+1}} Z(x_{TC}, \tau) d\tau \quad (21)$$

$\lambda$  being the material thermal conductivity and  $Z$  a function in the time domain obtained after using the Stehfest algorithm [31] for the Laplace transform inversion of the expression below:

$$Z = \mathcal{L}^{-1} \left\{ \frac{1}{\sqrt{\frac{p}{\alpha}}} \left[ \frac{\cosh\left(\sqrt{\frac{p}{\alpha}} L\right)}{\sinh\left(\sqrt{\frac{p}{\alpha}} L\right)} \cosh\left(\sqrt{\frac{p}{\alpha}} x_{TC}\right) - \sinh\left(\sqrt{\frac{p}{\alpha}} x_{TC}\right) \right] \right\} \quad (22)$$

200 where  $p$  is the Laplace variable.

Figure 5 presents the calibration data, which is a 50 s step input resulting in an increase and a subsequent decrease in the temperature at the probe location, and the two validation data with both positive and negative values of heat flux, the first being a sequence of different input functions and the second a sequence of step inputs with different widths. Actually, the ideal calibration input would be a Dirac pulse because it covers the entire frequency spectrum with the same amplitude, which means that all the phenomenon frequencies would be uniformly represented by the input signal. However, using a Dirac pulse in real systems, especially in heat transfer applications, is not always feasible because either the system input can only be applied for more than a minimum duration (so it is not a pulse) or the Dirac pulse results in a negligible output response. For this reason, using a step function is more representative of real systems applications but it contains more low-frequency signals, as shown in the frequency spectra in Fig. 6 (named "calibration (no filtering)"). In the same figure, we present as well the frequency spectra of the validations, which are as well more representative for lower frequencies, and a case of the calibration input with filtering, which is presented and discussed later. The geometry, probe location, material properties and time step used in this test case are available in Table 1. These values were chosen to simulate an experiment using a 20-mm thick nickel plate instrumented with a thermocouple inserted as close as possible to the surface where heat exchange occurs and with a data acquisition rate of 50 Hz (this is the reason of Fig. 6 ending at 25 Hz, which is the Nyquist frequency).

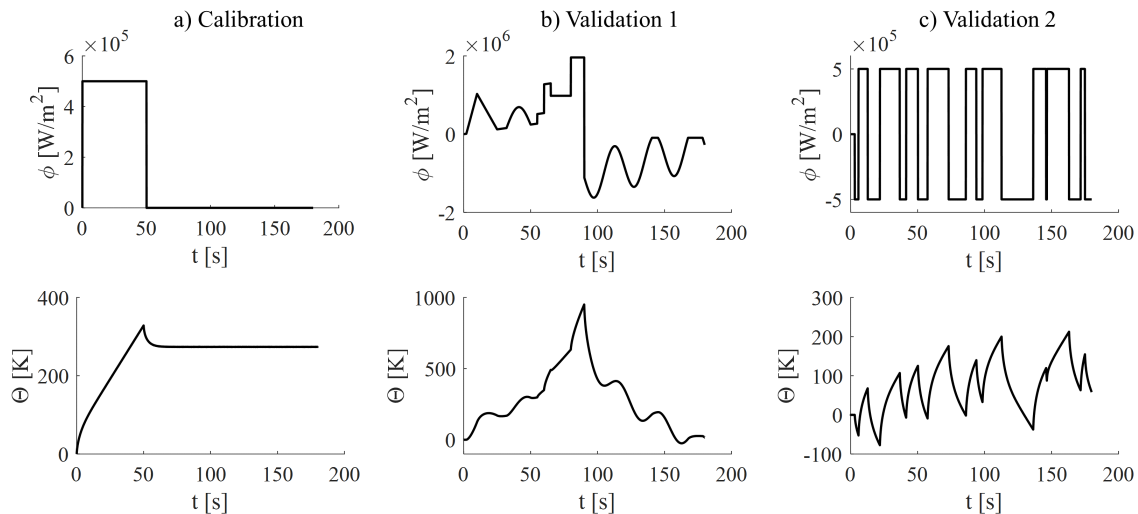


Figure 5: Inputs and outputs used for the calibration and validation steps (reference).

### 3.2. IARX calibration and validation

First, we perform the calibration step using the referential data for the input heat flux and temperature evolution in Fig. 5a to obtain the IARX parameters using least squares (Eq. 15). For this first analysis, we arbitrarily fixed the number of IARX parameters as  $n_a = n_b = n_c = 20$  and the temperature measurements contained a white noise with  $\sigma_\varepsilon = 1.10^{-5}$  K, i.e. nearly noiseless. Although in real experiments we would always have measurement noises, testing a noiseless case allows us to evaluate at first the IARX performance in an idealized condition, which is the case, for example, of numerical simulations. Then, the IARX method was validated using the temperature data presented in Fig. 5b and c and comparing the estimated and the referential heat fluxes. Figure 7 presents the results of both

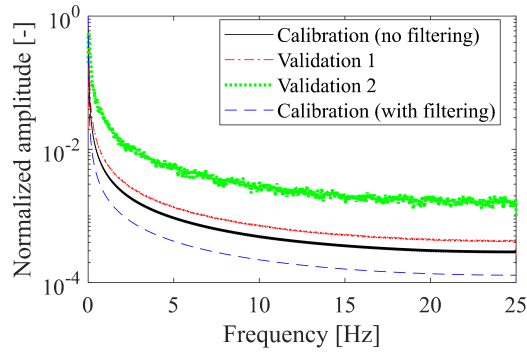


Figure 6: Normalized frequency spectra of the different inputs used in this study (smoothed using 20 neighboring points).

Table 1: Geometry, probe location and material properties used in the test cases.

Calculation parameters	Value
Wall dimension ( $L$ )	20 mm
Probe location ( $x_{TC}$ )	1 mm
Density ( $\rho$ )	8700 kg/m <sup>3</sup>
Specific heat ( $c_p$ )	525 J/(kg.K)
Thermal conductivity ( $\lambda$ )	52 W/(m.K)
Thermal diffusivity ( $\alpha$ )	1.1385.10 <sup>-5</sup> m <sup>2</sup> /s
Time step ( $\Delta t_k$ )	0.02 s

the calibration and validation steps. The input heat flux is well estimated for all the cases, with a mean residue  $\overline{|r|}$  lower than 1% for the calibration data set and lower than 3% for both the validations. We should remark that the relative residue is incalculable when the referential heat flux is zero (Eq. 17), which explains why there is no residue in the calibration results after 50 s. The highest residue of approximately 20% is observed in the first validation case at about 145 s and 176 s. This happens because the referential heat flux is the lowest in magnitude (about 9.10<sup>-4</sup> W/m<sup>2</sup>), so the relative error becomes higher. For the other points, the deviation between estimated and referential heat flux is not higher than 5%, hence the IARX succeeded to obtain the input heat flux even where there were large and discontinuous variations.

Nevertheless, in the case there is a noise with  $\sigma_\varepsilon = 1$  K standard deviation in the referential temperature, the IARX accuracy is largely degraded, as we observe in Fig. 8. Already in the calibration process, the IARX does not present a satisfactory result in estimating the input heat flux, with mean and maximum residues of 12.9% and 30%, respectively. This is even more evident in the validation process where both cases presented poor fit percentages (below 90%). The relative residues are poor as well, especially in the first case where the mean residue is higher than 64% and local deviations reach values above 400%. In the second validation test, the largest deviations are observed in the discontinuities, which could be tolerable for some applications. However, relative residues as high as 60% are still present in the middle of some steps, either overestimating and underestimating, which is hardly acceptable.

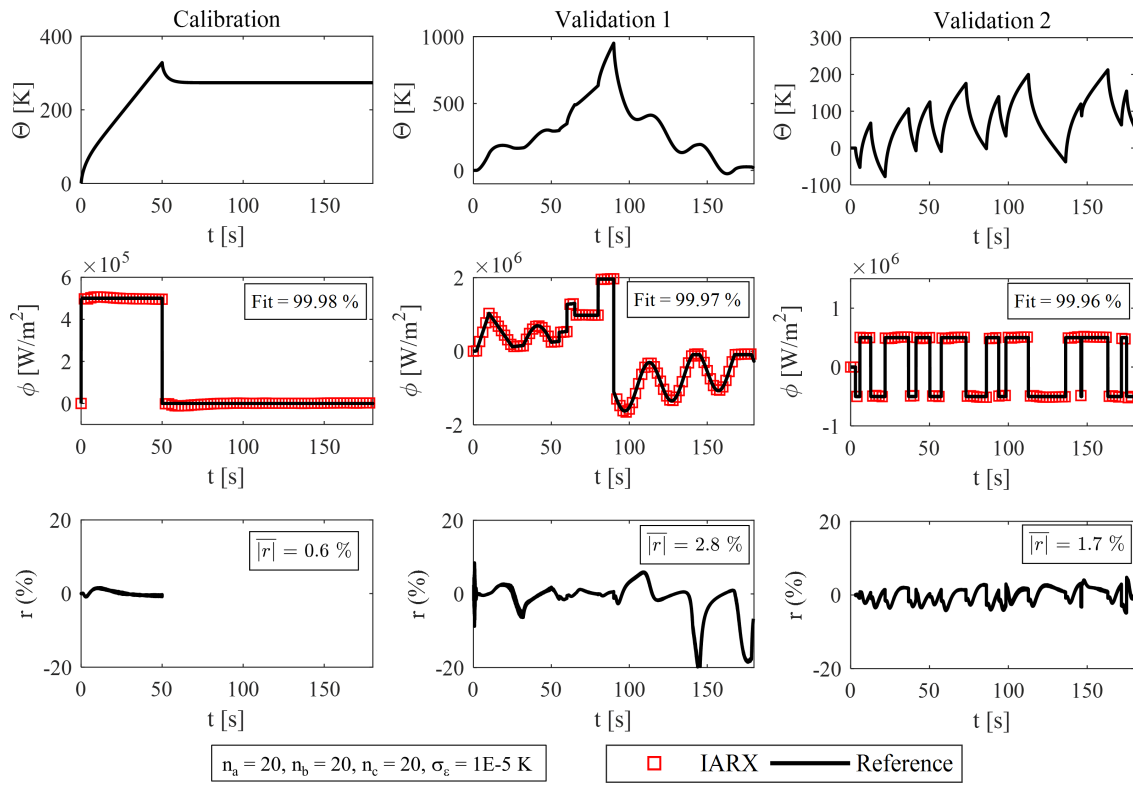


Figure 7: IARX calibration and validation with nearly noiseless temperature outputs.

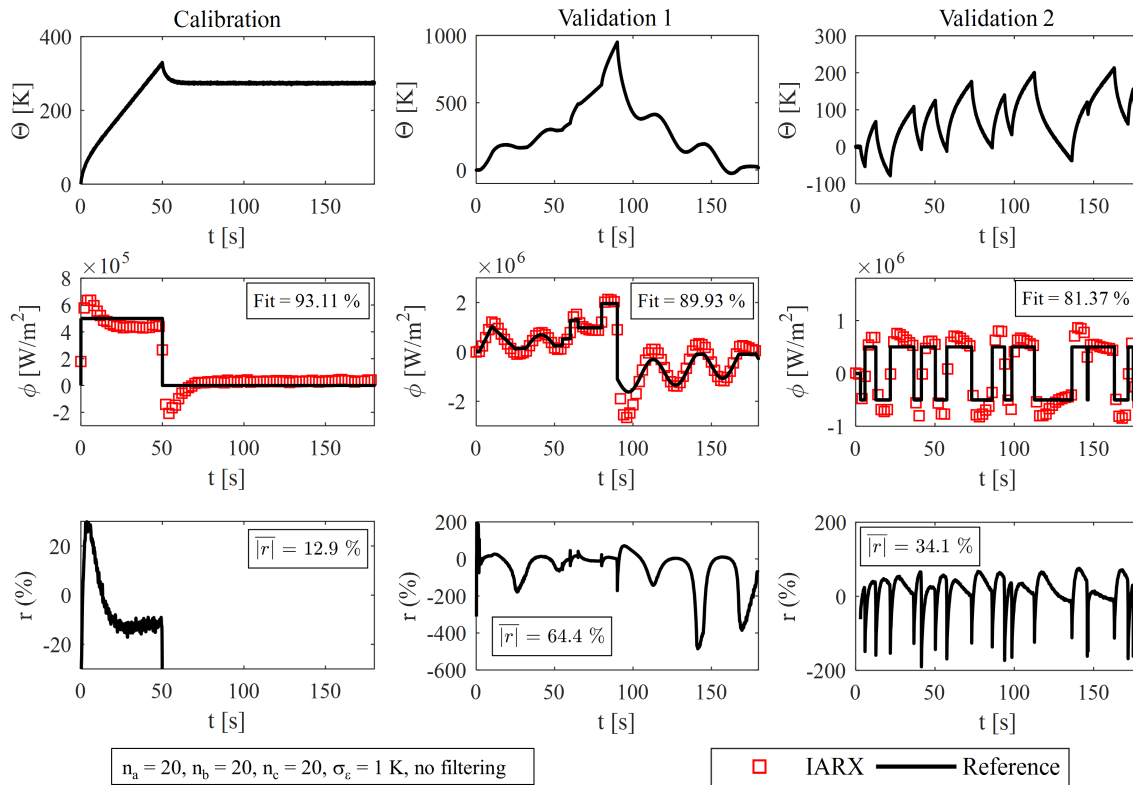


Figure 8: IARX calibration and validation with noisy temperature outputs and no filtering.

240 We could improve the IARX accuracy by increasing the number of parameters, but not excessively otherwise IARX would model the noise. However, it is preferable to use as few parameters as possible to work with a simpler model. One solution is reducing the temperature noise by filtering or smoothing only the calibration data to improve the parameters estimation. In this study, we used a convolution filtering on both the input and output that simply resulted in the cumulative summation of the signals. The main advantage of this method is the elimination of the

245 noise as the cumulative summation step increases because the mean value of the noise is zero (characteristic of white noise) and, consequently, the calibration data becomes virtually noiseless. On the other hand, this filtering decreases the amplitude of higher frequencies in the input signal (Fig. 6), hence the IARX method will represent better the lower frequencies of the input and may lose accuracy in fast transitions or discontinuities. Figure 9 presents the IARX calibration and validation steps with noisy temperature signals (still  $\sigma_\varepsilon = 1$  K) but with filtered calibration data. The

250 results show that even though we have only filtered the calibration data, the IARX method still succeeded to estimate well the input heat flux in both validation cases. Also, this calibration data filtering improved substantially the model accuracy, reducing the mean residues to 10.4% and 6.8% for the first and second validation cases, respectively. As expected, large deviations are still present at the discontinuities; however, local relative residues are globally not higher than 10%, except where the input heat flux is the lowest in magnitude and, consequently, more affected by

255 the temperature noise (for example, at about 16, 140 and 170 s in the first validation case). We should note that a noise standard deviation of 1 K is usually very high in real applications. However, we chose this value to test our IARX method in more difficult conditions and it still performed well.

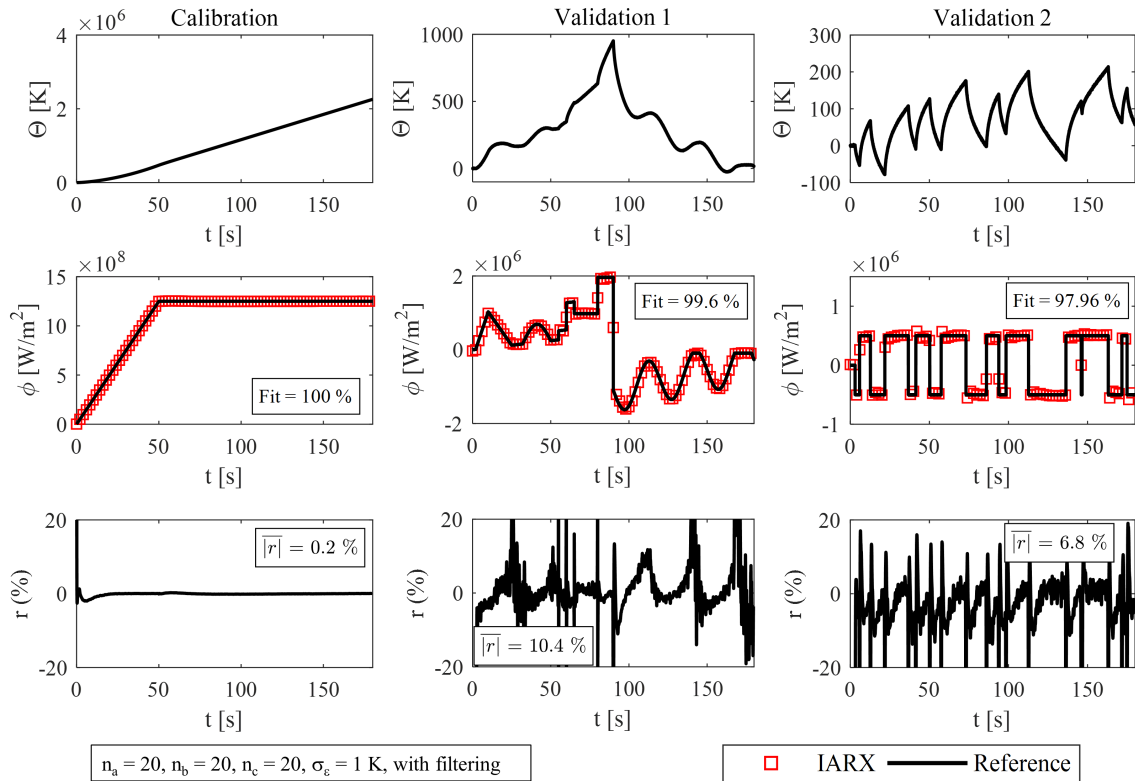


Figure 9: IARX calibration and validation with noisy temperature outputs and with filtering.

### 3.3. Analysis of the IARX parameters

For the analysis of each IARX parameter effect, we continued using a temperature noise of 1 K and we performed the calibration step using the aforementioned data filtering. Also, while varying the number of one type of IARX parameter to evaluate its effect, the number of the others were fixed to 20 (as before). At last, we present results in this section only with the first validation case to avoid overloading this article, but we tested as well the parameters effects with the second validation test and we reached the same results herein discussed.

Figure 10 presents the effect of the number of future exogenous parameters ( $n_c$ ) on the IARX results. First, estimating the input heat flux without future exogenous terms is unfeasible in the tested conditions as the calculation rapidly diverges. When using at least one future exogenous parameter, the IARX method provided a converging result even though it estimated poorly the input heat flux. Then, the increase in  $n_c$  improves the parametric model accuracy, reaching a satisfactory result with  $n_c = 10$  (fit = 99.1%). This analysis demonstrates the importance of  $n_c$  in the IARX estimation quality and that future exogenous parameters are indispensable to solve the inverse problem with the proposed method.

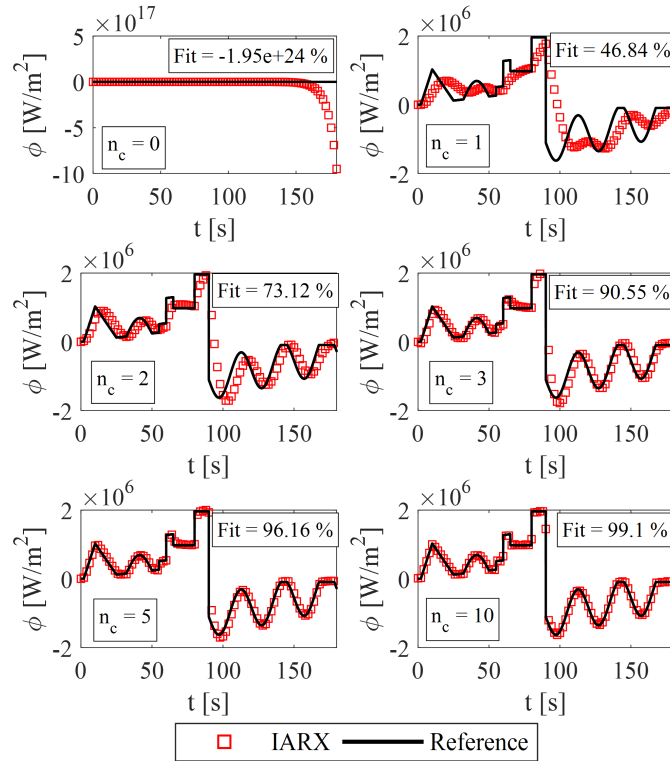


Figure 10: IARX results with the first validation case for different numbers of future exogenous parameters.

On the other hand, the number of past exogenous terms plays a minor, maybe negligible role on the parametric model estimation, as we see in Fig. 11. Even with  $n_b = 0$ , the inverse heat flux matched well the reference. This result is logical when reflecting on physics of the problem and causality principle. Because an input heat flux  $u[k]$  at a time step  $k$  only affects the system for future times, i.e. for  $t \geq t[k]$ , estimating  $u[k]$  using temperature information obtained in past times (when  $t < t[k]$ ) is unreasonable. That explains as well the previous result showing that the increase in the number of future exogenous terms improves the quality of the parametric model. Nevertheless, using a few past exogenous terms can improve a little the estimation of the input heat flux, as we see in Fig. 11, so its

use can be justified depending on the application and the desired model accuracy. Also, using both past and future exogenous terms might be useful in systems where it is difficult to identify which signals are inputs and which ones are outputs, a situation that can occur in complex multi-input-multi-output systems. The present study being a single-input-single-output system, the input (heat flux) and the output (temperature) are easily identified.

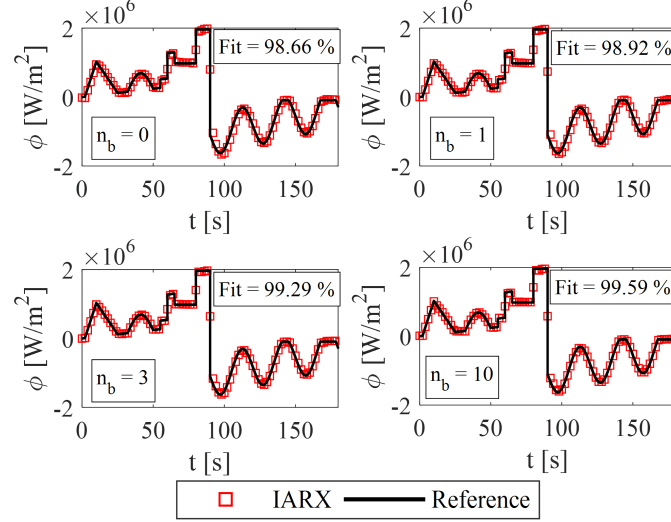


Figure 11: IARX results with the first validation case for different numbers of past exogenous parameters.

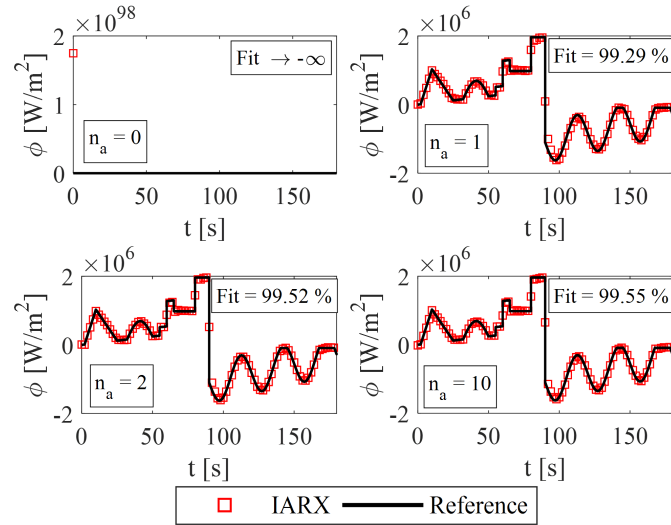


Figure 12: IARX results with the first validation case for different numbers of autoregressive parameters.

Finally, Fig. 12 presents how the number of autoregressive parameters affects the IARX results. When there are no autoregressive terms, the parametric model immediately diverges after a few time steps so the fit percentage tends to negative infinity. Using one autoregressive term is already sufficient to obtain fine estimations of the input heat fluxes, with a slight increase in the IARX quality using  $n_a = 2$ . However, a further increase in  $n_a$  does not increase any better the input heat flux estimation, as the fit percentage is practically the same for  $n_a = 2$  and  $n_a = 10$ . This happens because, for this test case, the method of least squares finds negligible values for  $a_i$  when  $i \geq 3$  (Fig. 13),  $a_1$  and  $a_2$  being the only autoregressive parameters that are significant to the parametric model either using or not past

exogenous terms ( $n_b = 20$  and  $n_b = 0$  in Fig. 13, respectively). One important characteristic in the IARX parameters is that, for any test case, number of parameters ( $n_a$ ,  $n_b$  and  $n_c$ ) or noise standard deviation, we always find that  $\sum a_i \approx -1$  and  $\sum b_i + \sum c_i \approx 0$ . Therefore, there is a compensation effect, which is common in parametric models, that tend to respect this condition, which is important to ensure IARX is still capable to estimate the heat input in steady-state conditions, even when the system is no longer at the same as the initial (like the calibration case).

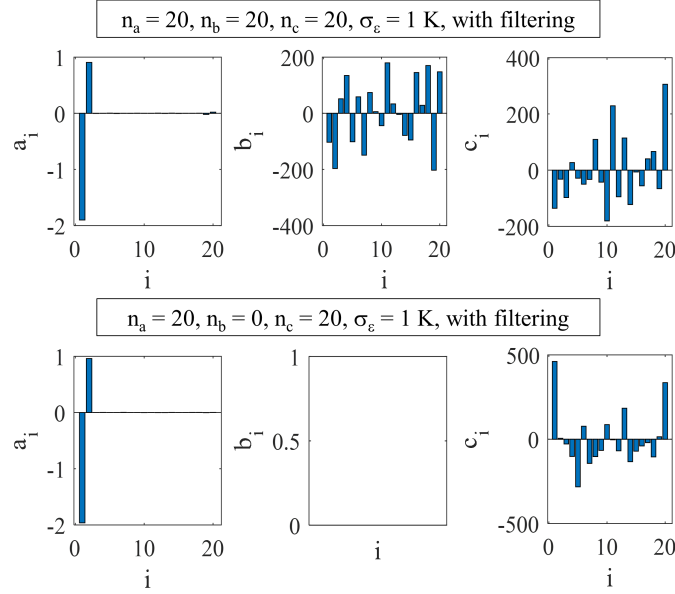


Figure 13: IARX parameters with and without past exogenous terms.

### 3.4. IARX vs. Beck's function specification method

In this section, we used the first validation case to compare the proposed IARX method to Beck's FSM, highlighting the advantages and disadvantages of each one. We applied data filtering in the calibration step to estimate the IARX parameters and, for both models, the temperature signals contain a white noise with  $\sigma_\epsilon = 1$  K.

Starting with the methods accuracy, Fig. 14a presents the mean residue of the models as a function of the number of future exogenous  $n_c$  in IARX and of the number of future time steps  $n_{fts}$  in FSM since these two parameters give the number of future data used to solve the IHCP. The number of autoregressive and past exogenous parameters in IARX was fixed to  $n_a = 2$  and  $n_b = 3$  to ensure a better input heat flux estimation with the least parameters, as demonstrated in the previous section. With both models, we observed a rapid decrease in the residue with the increase in the number of future data up to  $n_c = n_{fts} = 20$ , the FSM presenting a slightly steeper decrease compared to the IARX method. This information is important for real-time calculations or onboard diagnosis systems because using less future data to estimate a past input means a smaller delay in the calculated heat flux. For instance, a 10% mean residue is reached with  $n_{fts} = 15$  and  $n_c = 20$  using the FSM and the IARX, respectively. Therefore, if both models demanded the same computational time (which is not the case, as discussed further), the FSM would respond 0.1 s faster than the IARX for our test case (time step of 0.02 s, as shown in Table 1).

Nevertheless, a continued increase in the number of FSM future time steps results in an increase in the model residue. This occurs because the FSM hypothesis of future heat fluxes being equal to the calculated heat flux is untrue

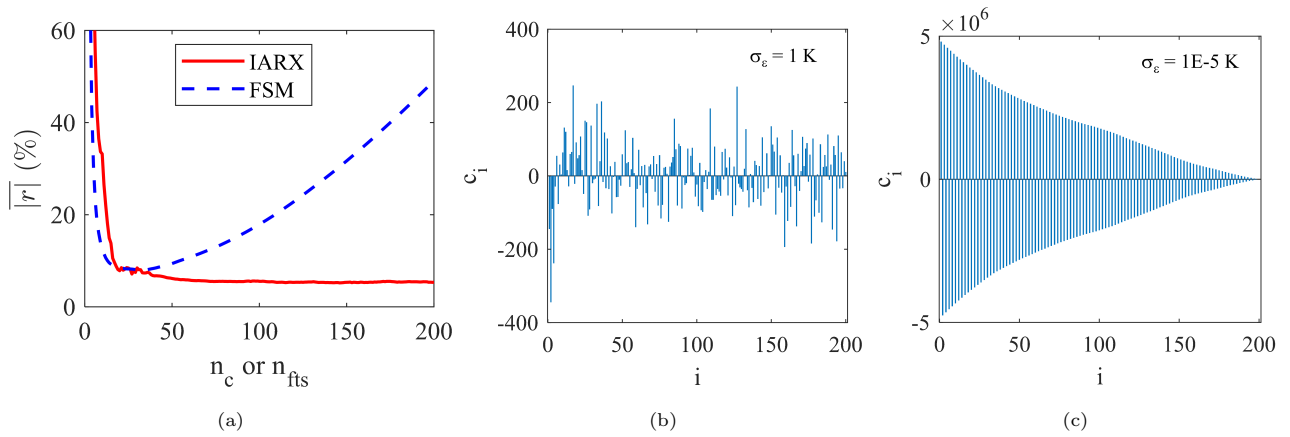


Figure 14: a) Mean residue as a function of the number of future exogenous parameters with IARX ( $n_c$ ) or future time step with FSM ( $n_{fts}$ ); b) IARX future exogenous parameters with  $n_c = 200$  for the tested case with  $\sigma_\epsilon = 1 \text{ K}$ ; c) IARX future exogenous parameters with  $n_c = 200$  for the tested case with  $\sigma_\epsilon = 1\text{E-}5 \text{ K}$ .

when the number of future time steps is excessive, resulting in a biased input estimation. On the other hand, this loss of accuracy does not occur with the IARX method when  $n_c$  is very large. One could imagine that this characteristic would occur because the highest order parameters would be negligible, as the heat equation is a parabolic differential equation. However, Fig. 14b shows the future exogenous parameters estimated by IARX using  $n_c = 200$  and we find that their value does not decrease as their order increases. This is related to the aforementioned compensation characteristic that takes place especially in the presence of noisy data. If the calibration data were noiseless, we would observe a decrease in the future exogenous values with the increase in the parameter order (Fig. 14c). Also, this unbiased result even with  $n_c = 200$  confirms that the IARX equation is indeed obtained with the hypothesis we adopted of setting  $b_{f,i} = 0$  for  $1 \leq i \leq n_c$  in Eq. 5 to obtain Eq. 6. If the hypothesis were considering future heat fluxes  $u[k+i]$  equal to  $u[k]$  or to zero, as we mentioned in the presentation of the model, we would observe biasing with a further increase in  $n_c$  (as we saw with the FSM), but this is not the case as demonstrated in this analysis.

Next, Fig. 15 presents the relative residue of each model with the first validation case. The number of future data for the IARX and the FSM in this calculation was, respectively,  $n_c = 20$  and  $n_{fts} = 15$  to compare two conditions with similar mean residue, as mentioned before. We found that the IARX residue did not contain much noise but is slightly biased in transitions of the input heat flux, which is a typical disadvantage of parametric models. This happens because the input used in the calibration step is richer with lower frequencies (Fig. 6), so IARX represents better these lower frequencies and can present this bias in transitions. Meanwhile, the residue with the FSM was not biased but was noisier, which could be reduced by increasing the number of future time steps. However, its advantage of faster input calculation compared to IARX would no longer exist and we could bias the estimates as already discussed. We should note that the FSM solution does not present any bias because we used an analytical solution with perfectly-known parameters to its calculation, which means there are no errors in the model. However, idealizations (for example, assuming constant thermophysical properties) or imprecise values of parameters (like using properties values found in datasheets or use imprecise measurements of the probe position) introduce deterministic errors to the model, i.e. they would bias the estimated heat flux. This is an advantage of parametric models like IARX: the calibration step comprises some non-idealizations and assumptions in the calculation of the parameters,

eliminating most of the model errors.

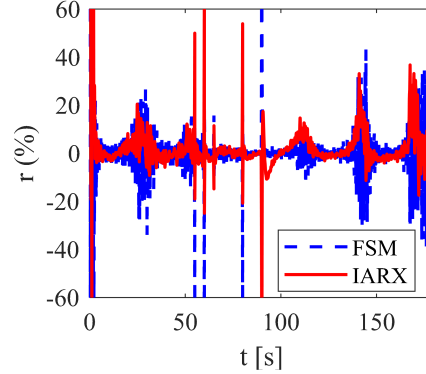


Figure 15: Comparison of the IARX and FSM residues using the first validation case with  $n_c = 20$  and  $n_{fts} = 12$ .

There are other important features related to their application that we must compare, especially considering computational costs. The following values herein presented were results of the calculations performed with MATLAB R2017b in a desktop computer with Windows 10 64-bits, Intel<sup>®</sup> Core<sup>™</sup> i5-7500 processor, 3.40 GHz base frequency, 16 GB RAM. Firstly, the FSM demands recording the entire history of the estimated heat fluxes and impedance (Eq. 21) to calculate the next input and, consequently, consumes more memory space. As an example of our test case, the input heat flux calculation at 40 s with the FSM required a stored data size of 96 kB (most part due to 6000 data from past heat fluxes and another 6000 data from the impedance). This amount of data obviously increases with the increase in the time step to be calculated. Meanwhile, for the same calculation, the IARX consumed only 400 B of memory space (200 B for the twenty-five IARX parameters, 160 B for the twenty future temperatures, 24 B for the three past temperatures and 16 B for the two past heat fluxes), without considering the calibration step which is necessary only once to obtain the parameters. These values for memory consumption may seem negligible compared to modern computers. Nevertheless, applications with onboard computing and diagnosis usually have very limited memory. For example, modern electronic control units (ECU) used in non-autonomous vehicles have about 2 to 8 MB memory capacity [32], hence consuming only hundreds of bytes instead of a hundred kilobytes is a substantial saving in memory space. One important advantage of the IARX method is that this memory consumption is constant for any time step calculation because we can discard temperature measurements and heat fluxes obtained before the time steps used in the past exogenous and autoregressive terms, respectively. For the same reason, the FSM requires a higher computational time than the IARX: respectively 212 and 117 ms to estimate all the heat fluxes in our test case, which means 45% reduction in calculation time if using IARX. Finally, we summarize in Table 2 the conclusions of the comparison between IARX and FSM with values from our test case between parentheses.

Table 2: Summary of the comparison between IARX and FSM.

Characteristic	IARX	FSM
Delay to estimate the input	Slightly larger (0.4 s)	Slightly smaller (0.3 s)
Excessive number of future data	No restriction (Fig. 14)	Substantially biased (Fig. 14)
Quality of the input estimate	Low noise, slightly biased (Fig. 15)	Locally noisy, no bias (Fig. 15)
Memory space	Smaller (400 B)	Larger (96 kB)
Calculation time	Faster (117 ms)	Slower (212 ms)

#### 4. Conclusions

This paper presented a novel method, named IARX (inverse ARX), to solve inverse heat conduction problems using a parametric model based on the classical ARX structure but containing future exogenous terms. The proposed model was validated using analytical solutions of a 1D heat conduction problem within a planar wall with one insulated surface and another with an imposed heat flux. By using the temperature evolution (the system output) at a given point within the wall, the IARX method was able to estimate successfully this input heat flux. For the tested cases without and with temperature noise, the model presented mean residue values of about 3% and 10%, although the latter required using a convolution filtering.

The analysis of the IARX parameters showed that the adoption of future exogenous terms plays an important role in the inverse problem solution and, moreover, in the model accuracy. Although using few past exogenous parameters slightly improves the model estimation, they are not necessary for the calculation, which is explained by the causality of the problem. Concerning the autoregressive parameters, at least one was necessary to obtain a converging result. With the tested case, only the first two autoregressive parameters were significant, while the others were very close to zero. Finally, a comparison was made between the IARX and Beck’s function specification method (FSM). On the one hand, Beck’s method presents unbiased but noisy estimates when using an optimized number of future time steps. On the other hand, the IARX estimates are less noisy but slightly biased, which is a typical disadvantage of parametric models, but using an excessive number of future exogenous parameter does not affect the model quality as we observe with the FSM. Also, IARX is computationally cost-effective as it requires much less memory space and its calculation is significantly faster.

#### 5. Future work

In this paper, we presented the novel IARX method and analyses of the model to understand how each parameter affected the inversion quality and how better could it be compared to a classical method like FSM, showing this is a promising tool, very useful for complex single-input-single-output systems. We expect to evaluate in future investigations how IARX works in other situations like with unfavorable instrumentation (a larger  $x_{TC}$ ), in 2D heat conduction problems or for multi-input-multi-output systems. This will allow understanding better the strengths and the limitations of the proposed method.

## 6. Acknowledgment

We would like to thank Prof. Denis Maillet from the LEMTA, Université de Lorraine, for the discussions and his  
385 intelligent and important remarks about our work.

## 7. Funding

This work was performed in the frame of the research project RESEM 2020, managed by the Institut de Recherche  
Technologique Matériaux Métallurgie Procédés (IRT M2P) and financially supported by the French program Plan  
d'Investissement d'Avenir (PIA).

## 390 References

- [1] D. Maillet, Y. Jarny, D. Petit, Problèmes inverses en diffusion thermique formulation et résolution du problème  
des moindres carrés, *Techniques de l'ingénieur Transferts thermiques* (2018) 1–21.
- [2] J. V. Beck, B. Blackwell, C. R. St. Clair Jr., *Inverse Heat Conduction: Ill-Posed Problems*, Wiley-Interscience  
publication, John Wiley & Sons, 1985.
- 395 [3] J. Beck, B. Blackwell, A. Haji-Sheikh, Comparison of some inverse heat conduction methods using experimental  
data, *International Journal of Heat and Mass Transfer* 39 (17) (1996) 3649 – 3657. doi:[https://doi.org/10.1016/0017-9310\(96\)00034-8](https://doi.org/10.1016/0017-9310(96)00034-8).
- [4] J. V. Beck, Nonlinear estimation applied to the nonlinear inverse heat conduction problem, *International Journal  
of Heat and Mass Transfer* 13 (4) (1970) 703 – 716. doi:[https://doi.org/10.1016/0017-9310\(70\)90044-X](https://doi.org/10.1016/0017-9310(70)90044-X).
- 400 [5] A. N. Tikhonov, V. Y. Arsenin, *Solution of ill-posed problems*, Winston, 1977.
- [6] A. Tikhonov, A. Goncharsky, V. Stepanov, A. G. Yagola, *Numerical Methods for the Solution of Ill-Posed  
Problems*, Vol. 328, Springer Netherlands, 2013. doi:10.1007/978-94-015-8480-7.
- [7] W. Hadad, D. Maillet, S. André, B. Rémy, Regularization using truncated singular value decomposition for  
estimating the fourier spectrum of a noised space distribution over an extended support, *Computer Assisted  
405 Methods in Engineering and Science* 21 (3/4) (2017) 211–222.  
URL <https://comes.ippt.pan.pl/index.php/comes/article/view/39>
- [8] P. C. Hansen, Truncated singular value decomposition solutions to discrete ill-posed problems with ill-determined  
numerical rank, *SIAM Journal on Scientific and Statistical Computing* 11 (3) (1990) 503–518. doi:<https://doi.org/10.1137/0911028>.
- 410 [9] M. Jahedi, F. Berntsson, J. Wren, B. Moshfegh, Transient inverse heat conduction problem of quenching a  
hollow cylinder by one row of water jets, *International Journal of Heat and Mass Transfer* 117 (2018) 748 – 756.  
doi:<https://doi.org/10.1016/j.ijheatmasstransfer.2017.10.048>.

- [10] B. Lamien, D. Le Maux, M. Courtois, T. Pierre, M. Carin, P. Le Masson, H. R. B. Orlande, P. Paillard, A bayesian approach for the estimation of the thermal diffusivity of aerodynamically levitated solid metals at high temperatures, *International Journal of Heat and Mass Transfer* 141 (2019) 265 – 281. doi:<https://doi.org/10.1016/j.ijheatmasstransfer.2019.06.054>.
- [11] C. P. Naveira-Cotta, R. M. Cotta, H. R. Orlande, Inverse analysis with integral transformed temperature fields: Identification of thermophysical properties in heterogeneous media, *International Journal of Heat and Mass Transfer* 54 (7) (2011) 1506 – 1519. doi:<https://doi.org/10.1016/j.ijheatmasstransfer.2010.11.042>.
- [12] S. Wan, P. Xu, K. Wang, J. Yang, S. Li, Real-time estimation of thermal boundary of unsteady heat conduction system using pid algorithm, *International Journal of Thermal Sciences* 153 (2020) 106395. doi:<https://doi.org/10.1016/j.ijthermalsci.2020.106395>.
- [13] M. N. Özisik, *Heat Conduction*, Wiley-Interscience publication, John Wiley & Sons, 1993.
- [14] L. Ljung, *System Identification: Theory for the User*, Prentice Hall PTR, 1999.
- [15] B. Milovanović, B. Božić, Z. Gospavić, M. Pejović, Comparison of ARX- and AR-models and of the assumed form of the transfer function when examining settlement of the building, in: 6th International Conference on Engineering Surveying (INGEO), Prague, Czech Republic, 2014.
- [16] M. Jiménez, M. Heras, Application of multi-output ARX models for estimation of the u and g values of building components in outdoor testing, *Solar Energy* 79 (3) (2005) 302 – 310. doi:<https://doi.org/10.1016/j.solener.2004.10.008>.
- [17] G. Mustafaraj, J. Chen, G. Lowry, Development of room temperature and relative humidity linear parametric models for an open office using bms data, *Energy and Buildings* 42 (3) (2010) 348 – 356. doi:<https://doi.org/10.1016/j.enbuild.2009.10.001>.
- [18] S. Wu, J.-Q. Sun, A physics-based linear parametric model of room temperature in office buildings, *Building and Environment* 50 (2012) 1 – 9. doi:<https://doi.org/10.1016/j.buildenv.2011.10.005>.
- [19] G. Ríos-Moreno, M. Trejo-Perea, R. C. neda Miranda, V. Hernández-Guzmán, G. Herrera-Ruiz, Modelling temperature in intelligent buildings by means of autoregressive models, *Automation in Construction* 16 (5) (2007) 713 – 722. doi:<https://doi.org/10.1016/j.autcon.2006.11.003>.
- [20] Y. Yu, D. Woradachjumroen, D. Yu, Virtual surface temperature sensor for multi-zone commercial buildings, *Energy Procedia* 61 (2014) 21 – 24, international Conference on Applied Energy, ICAE2014. doi:<https://doi.org/10.1016/j.egypro.2014.11.896>.
- [21] H. Yoshida, S. Kumar, Development of ARX model based off-line FDD technique for energy efficient buildings, *Renewable Energy* 22 (1) (2001) 53 – 59. doi:[https://doi.org/10.1016/S0960-1481\(00\)00033-1](https://doi.org/10.1016/S0960-1481(00)00033-1).
- [22] Y. Samyudia, H. Sibarani, Identification of reheat furnace temperature models from closed-loop data—an industrial case study, *Asia-Pacific Journal of Chemical Engineering* 1 (1-2) (2006) 70–81. doi:<https://doi.org/10.1002/apj.9>.

- [23] T. Loussouarn, D. Maillet, B. Remy, V. Schick, D. Dan, Indirect measurement of temperature inside a furnace, ARX model identification, in: 9th International Conference on Inverse Problems in Engineering (ICIPE), 2018. doi:<https://doi.org/10.1088/1742-6596/1047/1/012006>.
- 450 [24] B. Sahnoun, B. Remy, V. SCHICK, A. Lopez, R. Guilbaut, Modélisation et simulation du transfert thermique verre-moule dans un procédé de soufflage verrier, in: Congrès de la Société Française de thermique, Nantes, France, 2019.  
URL <https://hal.archives-ouvertes.fr/hal-02441357>
- [25] J.-L. Battaglia, L. Le Lay, J.-C. Batsale, A. Oustaloup, O. Cois, Utilisation de modèles d'identification non entiers pour la résolution de problèmes inverses en conduction, International Journal of Thermal Sciences 39 (3) 455 (2000) 374 – 389. doi:[https://doi.org/10.1016/S1290-0729\(00\)00220-9](https://doi.org/10.1016/S1290-0729(00)00220-9).
- [26] R. Malti, S. Victor, A. Oustaloup, Advances in system identification using fractional models, Journal of Computational and Nonlinear Dynamics 3 (2) (2008) 021401. doi:<https://doi.org/10.1115/1.2833910>.
- [27] T. A. Johansen, B. A. Foss, Empirical modeling of a heat transfer process using local models and interpolation, 460 in: Proceedings of 1995 American Control Conference, 1995, pp. 3654–3658. doi:<https://doi.org/10.1109/ACC.1995.533819>.
- [28] W. Al Hadad, Y. Jannot, D. Maillet, Characterization of a heat exchanger by virtual temperature sensors based on identified transfer functions, Journal of Physics: Conference Series 745 (2016) 032089.  
URL <https://doi.org/10.1088/1742-6596/745/3/032089>
- 465 [29] M. Gradeck, J. Ouattara, B. Rémy, D. Maillet, Solution of an inverse problem in the hankel space – infrared thermography applied to estimation of a transient cooling flux, Experimental Thermal and Fluid Science 36 (2012) 56–64. doi:<https://doi.org/10.1016/j.expthermflusci.2011.08.003>.  
URL <https://www.sciencedirect.com/science/article/pii/S0894177711001646>
- [30] D. Maillet, S. André, J. C. Batsale, A. Degiovanni, C. Moyne, Thermal Quadrupoles: Solving the Heat Equation 470 through Integral Transforms, John Wiley & Sons, 2000.
- [31] H. Stehfest, Algorithm 368: Numerical inversion of Laplace Transforms [d5], Commun. ACM 13 (1) (1970) 47–49. doi:10.1145/361953.361969.
- [32] M. Kaiser, U. Schaefer, G. Haaf, Electronic control unit, Springer Fachmedien Wiesbaden, Wiesbaden, 2015, pp. 18–43. doi:[https://doi.org/10.1007/978-3-658-03975-2\\_3](https://doi.org/10.1007/978-3-658-03975-2_3).

## 475 **Appendix A. Beck's function specification method**

Consider we are estimating the input heat flux  $\hat{\phi}[k]$  at the time step  $k$  and, for this purpose, all the previous heat fluxes are already known. Also, temperature measurements up to a time step  $k + 1 + n_{fts}$  are already available,  $n_{fts}$

being the number of future time steps. Hence, after using Eq. 20 to calculate  $\Theta[k+1]$  and isolating the term  $\hat{\phi}[k]$ , we obtain the following expression for the first future time step:

$$X_1 \hat{\phi}[k] = \Theta[k+1] - \sum_{j=0}^{k-1} X_{k-j+1} \hat{\phi}[j] \quad (\text{A.1})$$

480 Even very small temperature noises can make the heat flux estimation diverge rapidly. Hence, Beck proposed using equations that estimate future heat fluxes, which include future temperature measurements. However, because future heat fluxes are still unknown, we use the hypothesis considering future heat fluxes are equal to the heat flux to be estimated. Consequently, using again Eq. 20, we have the following equation for the second future time step:

$$X_1 \hat{\phi}[k+1] = \Theta[k+2] - X_2 \hat{\phi}[k] - \sum_{j=0}^{k-1} X_{k-j+2} \hat{\phi}[j] \quad (\text{A.2})$$

and considering  $\hat{\phi}[k+1] = \hat{\phi}[k]$ :

$$(X_1 + X_2) \hat{\phi}[k] = \Theta[k+2] - \sum_{j=0}^{k-1} X_{k-j+2} \hat{\phi}[j] \quad (\text{A.3})$$

485 We redo this calculation for the third future time step and we obtain the expression below:

$$X_1 \hat{\phi}[k+2] = \Theta[k+3] - X_2 \hat{\phi}[k+1] - X_3 \hat{\phi}[k] - \sum_{j=0}^{k-1} X_{k-j+3} \hat{\phi}[j] \quad (\text{A.4})$$

and considering  $\hat{\phi}[k+2] = \hat{\phi}[k+1] = \hat{\phi}[k]$ :

$$(X_1 + X_2 + X_3) \hat{\phi}[k] = \Theta[k+3] - \sum_{j=0}^{k-1} X_{k-j+3} \hat{\phi}[j] \quad (\text{A.5})$$

We can establish a pattern to find the equation for the  $n_{fts}^{th}$  future time step

$$\left( \sum_{j=1}^{n_{fts}} X_j \right) \hat{\phi}[k] = \Theta[k+n_{fts}] - \sum_{j=0}^{k-1} X_{k-j+n_{fts}} \hat{\phi}[j] \quad (\text{A.6})$$

This system of  $n_{fts}$  equations can be written in the matrix form as:

$$\mathbf{X}_{fts} \hat{\phi}[k] = \mathbf{d}_{fts} \quad (\text{A.7})$$

490 where  $\mathbf{X}_{fts}$  is the sensitivity vector built with the summation between parentheses in left of Eq. A.6 for each future time step, and  $\mathbf{d}_{fts}$  the result vector calculated as well for each future time step with the term in the right of Eq. A.6. Finally, we calculate  $\hat{\phi}[k]$  by the method of least squares, therefore:

$$\hat{\phi}[k] = \left( \mathbf{X}_{fts}^T \mathbf{X}_{fts} \right)^{-1} \mathbf{X}_{fts}^T \mathbf{d}_{fts} \quad (\text{A.8})$$

Now that  $\hat{\phi}[k]$  is known, as well as all the past heat fluxes (before the time step  $k$ ), we repeat the method to estimate the next heat flux  $\hat{\phi}[k+1]$ . This is performed progressively until the time step  $n_t - n_{fts}$  because there are no future temperature measurements to estimate heat fluxes after this point.